

## Rapid Communications

*The Rapid Communications section is intended for the accelerated publication of important new results. Since manuscripts submitted to this section are given priority treatment both in the editorial office and in production, authors should explain in their submittal letter why the work justifies this special handling. A Rapid Communication should be no longer than 3½ printed pages and must be accompanied by an abstract. Page proofs are sent to authors, but, because of the accelerated schedule, publication is not delayed for receipt of corrections unless requested by the author or noted by the editor.*

### Examination of the Cu/Si(111) 5×5 structure by scanning tunneling microscopy

R. J. Wilson and S. Chiang

IBM Almaden Research Center, San Jose, California 95120-6099

F. Salvan

Unité associée au Centre National de la Recherche Scientifique No. 783, Faculté des Sciences de Luminy,  
Département de Physique, Case 901, F-13288 Marseille Cedex 9, France

(Received 9 March 1988; revised manuscript received 25 May 1988)

The incommensurate 5×5 Cu/Si(111) structure has been examined by scanning tunneling microscopy. Images show that the surface structure is not well described as a hexagonal copper layer modulated at the Si(111) periodicity. Rather, the surface breaks up into 5×5 subunits which pack at spacings varying from 5 to 7 lattice constants, implying that substrate-adsorbate interactions dominate lateral interactions within the Cu adlayer.

The value of the scanning tunneling microscope (STM) for problems relating to the structure of ordered surfaces has already been established. In this paper, we present new results obtained for low-coverage Cu/Si(111) surfaces. When a copper layer is grown on clean Si(111) 7×7 surfaces at temperatures above a few hundred °C, an ordered, nearly 5×5 layer, has been observed.<sup>1-6</sup> This nearly 5×5 layer has been described as an incommensurate structure on the basis of low-energy electron-diffraction (LEED) observations of nonintegral order spots which fall between those expected for 5×5 and 6×6 geometries.<sup>3,4</sup> Incommensurate surfaces are formed when a mismatch exists in the lattice constant of a two-dimensional adsorbate layer ( $a_a$ ) relative to that of the substrate ( $a_s$ ), such that regular, repeating subunits are not formed.<sup>7</sup> The 5×5 layer is complete at Cu coverages of about 1 monolayer (ML), defined as 1 Cu atom per top layer Si atom. Further Cu deposition results in the appearance of alloy islands, nominally Cu<sub>3</sub>Si, coexisting with the 5×5 surface which takes on the role of an intermediate layer.<sup>2-4,8-10</sup> In order to understand the structure of this intermediate layer, we have examined the 5×5 structure with STM. Our results indicate that the pseudo-5×5 structure actually does involve nearly repetitive subunits which are irregularly spaced at lattice positions varying from 5 to 7 $a_s$ , where  $a_s = 3.84$  Å for the Si(111) surface. Our observations of this form of incommensurability are indicative of the wide range of different types of order which exist on real surfaces.

These measurements were performed with an ultrahigh-vacuum (UHV) STM system connected via a

sample transport chamber to a sample preparation and surface analysis system.<sup>11</sup> The Cu/Si(111) 5×5 structure was obtained by depositing slightly less than 1 ML of Cu, estimated from Auger data, on Si(111) 7×7 substrates, which had been prepared by repetitive heating to 1030 °C. The Si(111) substrate was held at about 650 °C during the 4-min evaporation period and for an additional 2 min following the deposition. The pressure did not exceed  $2 \times 10^{-10}$  Torr during the depositions. LEED patterns, for coverages slightly below 1 ML, typically showed mixed 5×5 and 7×7 structures, as expected.<sup>3</sup> STM observations also revealed regions of highly corrugated, pristine 7×7 and regions where a small corrugation, with a nominal 1×1 spacing, was observed. The 7×7 component of the LEED pattern was virtually extinguished, compared to the 5×5, for the sample which provided the images shown here.

The STM measurements described here were more difficult than for other ordered metal-semiconductor systems studied.<sup>12</sup> This is in part due to the small corrugations, typically 0.2 Å, and the requirement for high lateral resolution, ~2 Å, as shown in the STM image in Fig. 1(a). The images displayed have been processed on a mainframe computer to reduce noise, extend the number of pixels, enhance image contrast, and correct for instrumental drifts.<sup>13</sup>

Figure 1(b) shows a filled state image, obtained with tunnel current  $i_t = 2.0$  nA and tip bias  $V_t = +0.5$  V, for a relatively large area scan. The 1×1 corrugation, regions of hexagonally packed (HP) bumps, a partially ordered array of widely spaced triangular depressions (T), and

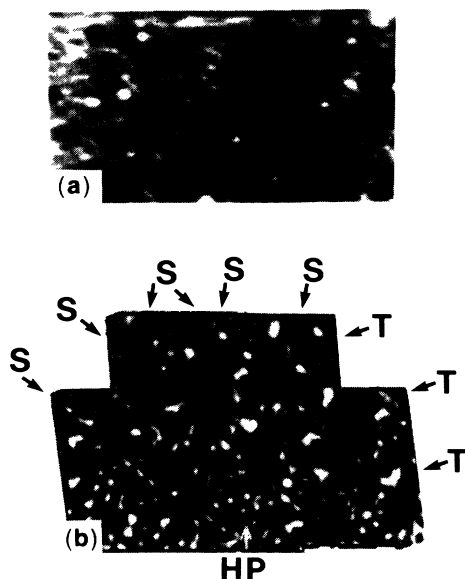


FIG. 1. (a) Gray scale top view image of filled states of  $\sim 115 \times 90 \text{ \AA}$  area of CuSi(111), recorded with  $V_t = +1.0 \text{ V}$  and  $i_t = 1.0 \text{ nA}$ , with no image processing other than subtraction of a background plane. (b) Composite image of  $\sim 120 \times 80 \text{ \AA}$  area of Cu/Si(111) 5×5 surface. Imaging conditions and identifying symbols are defined in the text. White represents features which appear elevated, and the full-scale corrugation is  $0.3 \text{ \AA}$ .

poorly resolved stripes (S) which extend across the image are evident. Although the strong irregularities in Fig. 1(b) suggest considerable noise in the STM data, this is not the case, since Fig. 1(b) is actually a composite image made by digitally superimposing three images which share an identifiable defect. The rms difference in apparent height in the overlap region amounts to only  $0.02 \text{ \AA}$ . Drift corrections and image registration were initially attempted by using a bilinear transformation to map the HP features onto hollow sites ( $H_3$ ) of the top-layer Si mesh which are not above second-layer Si atoms. Small corrections to this mapping were found to bring most of the observed protrusions onto nearly equivalent sites on the Si(111) mesh as shown in Fig. 2(a). The triangular features map very reproducibly onto equivalent positions. Although the simplest interpretation of the image is that the observed protrusions represent individual Cu atoms occupying most of the available hollow sites, we cannot unambiguously determine the type of atom from these measurements.<sup>12,14</sup> Alternatively, it can be argued that the image represents top-layer Si atoms perturbed by Cu insertion into the surface. With this reservation, the assignment of the protrusions to  $H_3$  sites has been made on the basis of Auger electron diffraction analysis of the Cu binding site.<sup>5</sup> Figure 2(a) also illustrates how the image can be decomposed into irregular 5×5 subunits. Although some features in the three-dimensional view in Fig. 2(b) show departure from threefold symmetry, the data vary with voltage and also with tip characteristics. We have not observed abrupt domain boundaries between 7×7 and 5×5 regions which would allow us to determine the relative registration of the two structures,<sup>12</sup> even

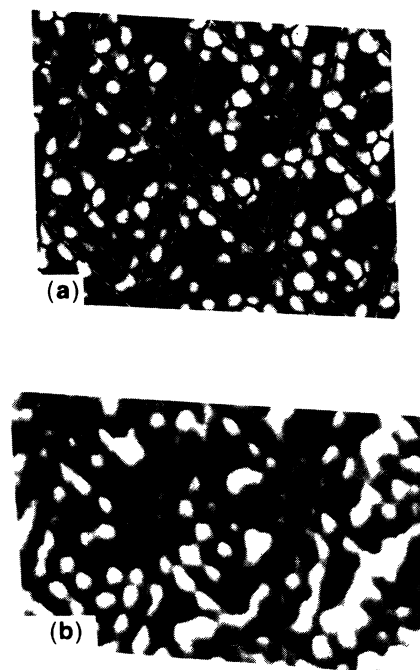


FIG. 2. (a) STM image of  $\sim 57 \times 47 \text{ \AA}$  area, showing same area as lower middle part of Fig. 1(b), recorded with  $V_t = +0.5 \text{ V}$  and  $i_t = 2.0 \text{ nA}$ . The data have been overlaid with a black Si(111) mesh, where open (closed) circles represent first (second) layer Si atoms. White dashed lines show a decomposition of the image into 5×5 cells and domain walls. (b) A three-dimensional perspective view of the same 5×5 region as in (a), emphasizing the internal structure of the cell.

though clean Si(111) 7×7 and Cu/Si(111) 5×5 areas were observed on nearby terraces.

To determine the size of the mesh which best fits the adsorbate structure, we mapped a Si(111) 7×7 image, obtained within  $3 \mu\text{m}$  of the Cu/Si(111) 5×5 region shown in Fig. 1, onto the same ideal Si(111) mesh which we have used in Fig. 2(a). Using the dimer-adatom-stacking fault model for the 7×7 structure,<sup>15</sup> the Si adatoms are placed onto their correct lateral sites relative to the unreconstructed Si(111) mesh. Figure 3 shows images of 5×5 and 7×7 regions which were each corrected for drifts and registered with hexagonal meshes. Using the appropriate scan widths for the images, the mesh which best fits the adsorbate structure has the size ratio of  $0.95 \pm 0.07$  relative to the mesh which best fits the 7×7 structure. Analysis of LEED patterns in terms of a simple incommensurate overlayer, however, gives the size ratio of these lattices to be  $0.816 \pm 0.003$ .<sup>3,4</sup> We thus conclude that the simple picture of a gently modulated hexagonal Cu adlayer is inappropriate. Theoretical first-principles calculations indicate that Cu atoms bonded to a Si(111) surface have a higher chemisorption energy and a significantly lower penetration barrier than Ag on the same surface.<sup>16</sup> These differences suggest that Cu atoms are pulled by strong substrate interactions into a nearly 1×1 arrangement on Si(111), while the mean spacing of Ag atoms of the  $\sqrt{3}$  Ag/Si(111) is considerably larger.<sup>12</sup> Figure 3 also illustrates the difficulty of observing STM images on the

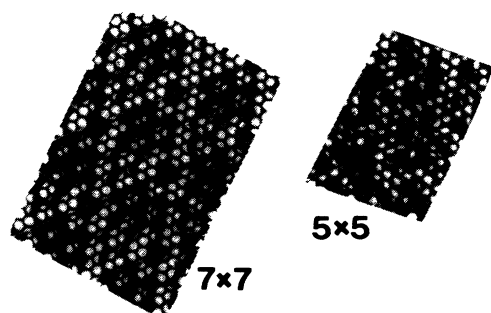


FIG. 3. STM images of  $7 \times 7$  and  $5 \times 5$  portions of the surface, after mapping onto the Si(111) mesh. The unit-cell edge of the  $7 \times 7$  is  $26.9 \text{ \AA}$  and that of the  $5 \times 5$  is  $19.2 \text{ \AA}$ . The scan widths are about  $60$  and  $40 \text{ \AA}$ , respectively. The total gray scale range for the  $7 \times 7$  image is  $\sim 2 \text{ \AA}$ , and that for the  $5 \times 5$  image is  $\sim 0.2 \text{ \AA}$ .

Cu/Si(111)  $5 \times 5$  surface as compared to the  $7 \times 7$  surface in that the lateral resolution must be significantly better and the vertical sensitivity is increased by a factor of 10.

The observation of a mesh compatible with Si(111) requires a strong substrate-adsorbate coupling view of the incommensurability observed here. We then interpret our images in terms of an incommensurate layer which breaks up into small patches, which are centered near regions of favorable registration, to relieve strains associated with the lattice mismatch. The relatively good long-range order and the registration degeneracy of the stable triangular subunits are understood in terms of global strain relief and local bonding sites, respectively.

The images expected for an incommensurate structure can take many forms. Figure 4 shows the interaction of Cu atoms with a periodic potential as the substrate-adsorbate interaction is increased. Figure 4(a) shows the one-dimensional case for which the Cu atoms are regularly spaced with no interaction between substrate and adsorbate atoms. As the substrate-adsorbate interactions are increased relative to the intralayer interactions of the adlayer, it becomes unfavorable for Cu atoms to occupy, for example, an atop site. The Cu adlayer will be modulated spatially by the periodic potential, both laterally and vertically, as shown in Fig. 4(b). In the limit where substrate-adsorbate interactions dominate, the adatoms should all appear very near the optimal hollow adsorption sites, as in Fig. 4(c). One then obtains nearly commensurate domains broken up by domain walls, indicated by arrows, which can render the overall structure incommensurate. In two dimensions, typical symmetry and binding-site variations are shown in Fig. 4(d), which has an incommensurate superposition of two threefold lattices with  $\sim 20\%$  misfit. Note that the positions where the adlayer sites closely match the binding site are quasiperiodic and somewhat ambiguous. Breakup of the overlayer into nearly commensurate cells separated by domain walls can be easily visualized. The striplike features are strikingly similar to those seen in Fig. 1.

One should also consider the atomic arrangements for the Cu-Si alloy island phase as a possible explanation for

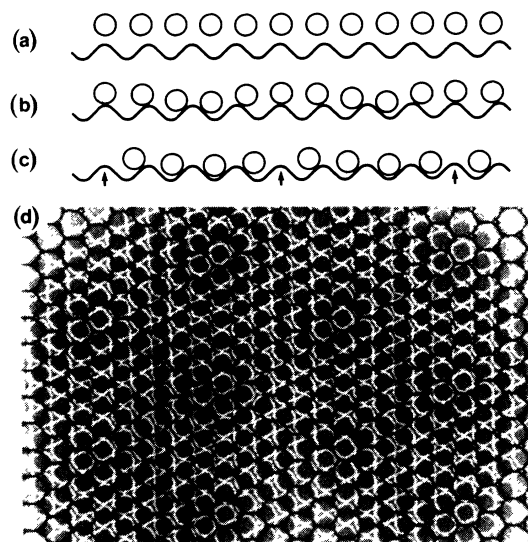


FIG. 4. (a) Surface potential diagram and Cu adatom positions for a hypothetical 1D incommensurate Cu/Si(111) surface with no interlayer interactions. (b) As the substrate-adsorbate interactions are increased, the Cu adlayer is modulated by the Si lattice periodicity. (c) For substrate-adsorbate interactions dominating the Cu-Cu interaction, the adsorbate layer breaks up into domains dominated by favorable hollow binding sites, separated by walls, indicated by arrows. This behavior is expected for a 1D incommensurate structure. (d) Incommensurate superposition of two threefold lattices with  $\sim 20\%$  misfit, showing the symmetry and binding-site variations in two dimensions.

the  $5 \times 5$  cells. The structure of the polymorphic  $\text{Cu}_3\text{Si}$  phases which comprise the alloy islands have been deduced from transmission electron diffraction measurements.<sup>17</sup> From these measurements it is known that the alloy is comprised of three stacked HP layers. Two of these layers are pure Cu and the third is a mixed Cu-Si layer. These layers stack parallel to the  $(1\bar{1}1)_{\text{Si}}$  plane with  $(111)_{\text{Si}} \parallel (089)_{\eta''}$ . This gives a good match to the (111) Si spacing with the projected  $\eta''$  lattice being about 5% larger than the Si(111) mesh.<sup>18</sup> However, the inclination of the layer axis with respect to the Si(111) normal ensures that planes parallel to the surface contain both Cu and Si atoms. Although we do not expect the first layer of Cu to take up the bulk alloy structure, the above considerations strengthen our reservations regarding the literal interpretation of our images in terms of only Cu or only Si atoms.

It is not difficult to reconcile our measurements with LEED observations. Indeed the surface order is close to  $5 \times 5$  with gaps between many of the cells. The relatively good long-range order is, in the present case, manifested by the stripes in Fig. 1(b) which appear quite continuous in spite of the erratic positioning of the triangular sites. Since LEED spot intensities represent spatial averages over regions, the diffraction response depends critically on the form of the correlation function and is not inconsistent with our observations.<sup>19</sup> Similar statements apply to Auger electron diffraction determinations of  $H_3$  Cu bind-

ing sites,<sup>5</sup> which may well describe most of the sites within the 5×5 cell.

The problem for STM, at present, is that it is difficult to unambiguously identify the atomic species,<sup>12,14</sup> to separate geometric and electronic structure, or to identify subsurface rearrangements. These problems can be addressed by careful modeling and measurements but, at present, the 5×5 Cu/Si(111) structure observed here is too complex for unambiguous interpretations to be made. Bias-dependent STM measurements have also been carried out on this surface<sup>20</sup> and show the same types of features shown here. It is our hope that this analysis can proceed further when more electronic structure data are available from other techniques and STM of other metal-

semiconductor interfaces is better understood.

The results we have obtained clearly demonstrate that the Cu/Si(111) 5×5 surface is not a mildly perturbed hexagonally packed Cu layer. Substrate interactions strongly dominate, and the layer breaks up into irregularly spaced 5×5 cells. Although the images are consistent with Cu coverages near 1 ML, the Cu binding site is probably not unique, and specific sites, involving only a few atoms per 5×5 cell, are important for understanding the atomic details of this surface.

We wish to acknowledge helpful discussions with F. Abraham and assistance with computer programming from J. Shyu.

<sup>1</sup>J. T. Grant and T. W. Haas, *Surf. Sci.* **19**, 347 (1970).

<sup>2</sup>F. Ringeisen, J. Derrien, E. Daugy, J. M. Layet, P. Mathiez, and F. Salvan, *J. Vac. Sci. Technol. B* **1**, 546 (1983).

<sup>3</sup>E. Daugy, P. Mathiez, F. Salvan, and J. M. Layet, *Surf. Sci.* **154**, 267 (1985).

<sup>4</sup>H. Kemmann, F. Muller, and H. Neddermeyer, *Surf. Sci.* **192**, 11 (1987).

<sup>5</sup>S. A. Chambers, S. B. Anderson, and J. H. Weaver, *Phys. Rev. B* **32**, 581 (1985).

<sup>6</sup>H. Dallaporta and A. Cros, *Surf. Sci.* **178**, 64 (1986).

<sup>7</sup>J. Villain, in *Ordering in Strongly Fluctuating Condensed Matter Systems*, edited by T. Riste (Plenum, New York, 1980), p. 221.

<sup>8</sup>I. Abbati and M. Grione, *J. Vac. Sci. Technol.* **19**, 631 (1981).

<sup>9</sup>G. Rossi, T. Kendelewicz, I. Lindau, and W. E. Spicer, *J. Vac. Sci. Technol. A* **1**, 987 (1983).

<sup>10</sup>S. A. Chambers, G. A. Howell, T. R. Greenlee, and J. H. Weaver, *Phys. Rev. B* **31**, 6402 (1985).

<sup>11</sup>S. Chiang, R. J. Wilson, Ch. Gerber, and V. M. Hallmark, *J. Vac. Sci. Technol. A* **6**, 386 (1988).

<sup>12</sup>R. J. Wilson and S. Chiang, *Phys. Rev. Lett.* **58**, 369 (1987); **59**, 2329 (1987).

<sup>13</sup>R. J. Wilson and S. Chiang, *J. Vac. Sci. Technol. A* **6**, 398 (1988).

<sup>14</sup>E. J. Van Loenen, J. E. Demuth, R. M. Tromp, and R. J. Hamers, *Phys. Rev. Lett.* **58**, 373 (1987).

<sup>15</sup>K. Takayanagi, Y. Tanishiro, S. Takahashi, and M. Takahashi, *Surf. Sci.* **164**, 367 (1985).

<sup>16</sup>S.-H. Chou, A. J. Freeman, S. Grigoras, T. M. Gentle, B. Dellely, and E. Wimmer, *J. Am. Chem. Soc.* **109**, 1880 (1987).

<sup>17</sup>J. K. Solberg, *Acta Crystallogr. Sect. A* **34**, 684 (1978).

<sup>18</sup>G. Weber, B. Gillot, and P. Barret, *Phys. Status Solidi A* **75**, 567 (1983).

<sup>19</sup>R. L. Park and J. E. Houston, *Surf. Sci.* **18**, 213 (1969); **21**, 209 (1970); **26**, 269 (1971).

<sup>20</sup>U. K. Koehler and J. E. Demuth (private communication).

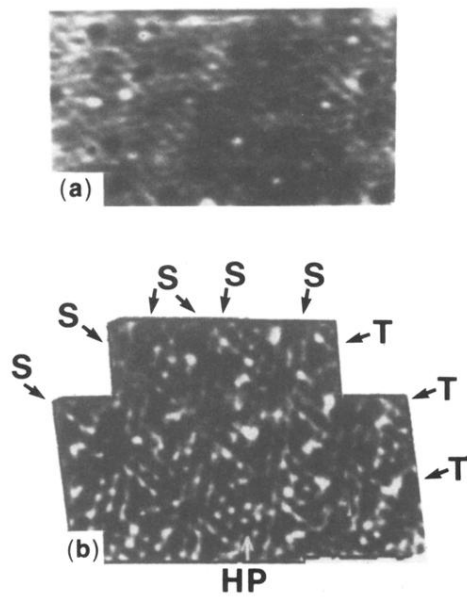


FIG. 1. (a) Gray scale top view image of filled states of  $\sim 115 \times 90 \text{ \AA}$  area of CuSi(111), recorded with  $V_t = +1.0 \text{ V}$  and  $i_t = 1.0 \text{ nA}$ , with no image processing other than subtraction of a background plane. (b) Composite image of  $\sim 120 \times 80 \text{ \AA}$  area of Cu/Si(111)  $5 \times 5$  surface. Imaging conditions and identifying symbols are defined in the text. White represents features which appear elevated, and the full-scale corrugation is  $0.3 \text{ \AA}$ .

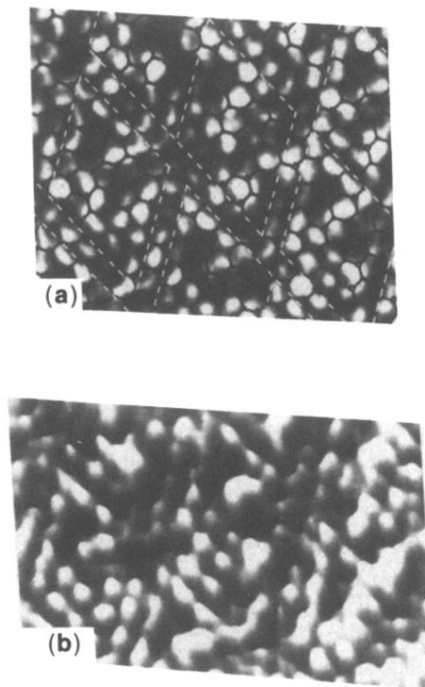


FIG. 2. (a) STM image of  $\sim 57 \times 47 \text{ \AA}$  area, showing same area as lower middle part of Fig. 1(b), recorded with  $V_t = +0.5 \text{ V}$  and  $i_t = 2.0 \text{ nA}$ . The data have been overlaid with a black Si(111) mesh, where open (closed) circles represent first (second) layer Si atoms. White dashed lines show a decomposition of the image into  $5 \times 5$  cells and domain walls. (b) A three-dimensional perspective view of the same  $5 \times 5$  region as in (a), emphasizing the internal structure of the cell.

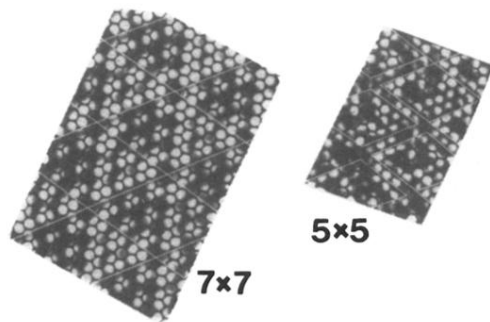


FIG. 3. STM images of  $7\times 7$  and  $5\times 5$  portions of the surface, after mapping onto the Si(111) mesh. The unit-cell edge of the  $7\times 7$  is  $26.9 \text{ \AA}$  and that of the  $5\times 5$  is  $19.2 \text{ \AA}$ . The scan widths are about  $60$  and  $40 \text{ \AA}$ , respectively. The total gray scale range for the  $7\times 7$  image is  $\sim 2 \text{ \AA}$ , and that for the  $5\times 5$  image is  $\sim 0.2 \text{ \AA}$ .

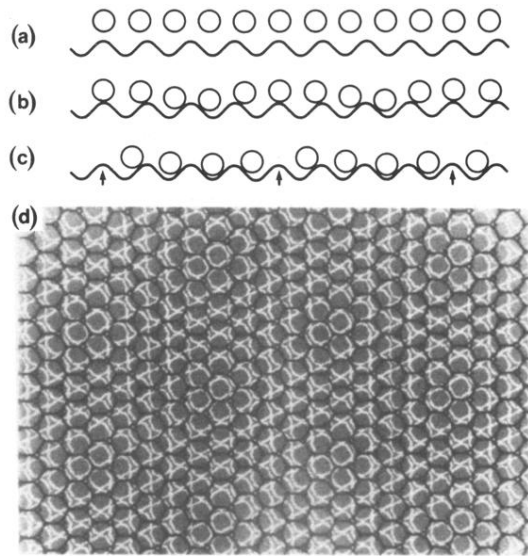


FIG. 4. (a) Surface potential diagram and Cu adatom positions for a hypothetical 1D incommensurate Cu/Si(111) surface with no interlayer interactions. (b) As the substrate-adsorbate interactions are increased, the Cu adlayer is modulated by the Si lattice periodicity. (c) For substrate-adsorbate interactions dominating the Cu-Cu interaction, the adsorbate layer breaks up into domains dominated by favorable hollow binding sites, separated by walls, indicated by arrows. This behavior is expected for a 1D incommensurate structure. (d) Incommensurate superposition of two threefold lattices with  $\sim 20\%$  misfit, showing the symmetry and binding-site variations in two dimensions.